International Journal of Mathematical Archive-9(10), 2018, 72-84
Available online through www.ijma.info ISSN 2229 – 5046

INFLUENCE OF THERMAL RADIATION, THERMO-DIFFUSION, RADIATION ABSORPTION ON MIXED CONVECTIVE HEAT AND MASS TRANSFER FLOW OF A MICROPOLAR FLUID IN A VERTICAL CHANNEL WITH VARIABLE TEMPERATURE IN THE PRESENCE OF HAT SOURCES

DR. C. VENKATALAKSHMI[1] AND LAKSHMI REDDY*[2]

[1]Assistant Professor,
Department of Applied Mathematics,
Sri Padmavathi Mahila University, Tirupati, (A.P.), India.

[2]Research Scholar,
Department of Applied Mathematics,
Sri Padmavathi Mahila University, Tirupati, (A.P.), India.

(Received On: 17-08-18; Revised & Accepted On: 04-10-18)

ABSTRACT

We analyze the combined influence of chemical reaction, thermal radiation, radiation absorption, Soret and Dufour effects on mixed convective heat and mass transfer flow of a micropolar fluid between two vertical parallel plates with varying temperature in the presence of heat sources. Such type of study may be applicable in nuclear reactors, heat exchangers and various electronic devices.

Keywords: *Thermal Radiation, Soret and Dufour effect, Radiation Absorption, Vertical Channel, Chemical Reaction.*

1. NTRODUCTION

The study of non-Newtonian fluid flows has gained much attention from researchers because of its applications in biology, physiology, technology and industry. In addition, the effects of heat and mass transfer in non-Newtonian fluid also have great importance in engineering applications such as thermal design of industrial equipment dealing with molten plastics, polymeric liquids, foodstuffs, or slurries. Several investigators have extended many of the available convection heat and mass transfer problems to include the non-Newtonian effects. Many of the non-Newtonian fluid models describe the nonlinear relationship between stress and the rate of strain. But the micropolar fluid model introduced by Eringen [6] exhibits some microscopic effects arising from the local structure and micro motion of the fluid elements. Further, they can sustain couple stresses and include classical Newtonian fluids as a special case. The model of micropolar fluid represents fluids consisting of rigid, randomly oriented (or spherical) particles suspended in a viscous medium where the deformation of the particles is ignored. Micropolar fluids have been shown to accurately simulate the flow characteristics of polymeric additives, geomorphological sediments, colloidal suspensions, hematological suspensions, liquid crystals, lubricants etc. The mathematical theory of equations of micropolar fluids and applications of these fluids in the theory of lubrication and porous media is presented by Lukaszewicz.

Eringen [6] introduced the concept of micro fluids, which deals with a class of fluids, exhibiting certain microscopic effects arising from the local structure and micro-motions of the fluid elements. These fluids can support stress moments and body moments and body moments and are influenced by the spin inertia. Later, Eringen [7] developed a subclass of these micro fluids, called micropolar fluids, where the micro-rotational effects and micro-rotational inertia exist but they do not support stretch. They can support couple stresses and body couples only. Physically some polymeric fluids, fluids containing small amounts of polymeric additives, blood, paints, lubricating oils, liquid crystals, colloidal fluids and suspension fluid may be represented by the mathematical model, underlying micropolar fluids. An excellent review of micropolar fluids and their applications were provided by Ariman *et al.* [3]. Hoyt and Fabula [9] have shown experimentally that the fluids containing minute polymeric additives indicate considerable reduction of the skin friction (about 25–30%); a concept, which is well explained by the theory of micropolar fluids. As an application, these fluids with microstructure are also capable of representing the body fluids.

Corresponding Author: Lakshmi Reddy*[2]
[2]Research Scholar, Department of Applied Mathematics,
Sri Padmavathi Mahila University, Tirupati, (A.P.), India.

The problems of micropolar fluid flow between two vertical plates (channel) are of great technical interest. A lot of attention has been given by many researchers. Sastry and Rao [15] have studied the effect of suction in the laminar flow of a micropolar fluid in a channel, considering the Poiseuille flow at the entry of the channel. Bhargava and Rani [4] have examined the convective heat transfer in micropolar fluid flow between parallel plates. Its extension to free and forced convection is an interesting area of research including liquid crystals, dilute solutions of polymer fluids and many types of suspensions, since in many configurations in the technology and nature, one continually encounters masses of fluid rising freely in an extensive medium due to the buoyancy effects. Agarwal and Dhanapal [2] analyzed free convection micropolar fluid flow between two parallel porous vertical plates. The problem of fully developed free convection of a micropolar fluid in vertical channels has been discussed by Chamkha *et al.* [5]. Srinivasacharya *et al.* [17] have investigated the problem of unsteady stokes flow of micropolar fluid between two parallel porous plates. In a forced convection situation, natural convection effects are also present in the presence of gravitational body forces. The situation where both the natural and forced convection effects are of comparable order is called mixed or combined convection. Gorla *et al.* [8] studied the fully developed laminar mixed convection flow of a micropolar fluid between two vertical parallel plates maintained at uniform but different temperatures. Excellent applications can be found in Nigam *et al.* [13], where the authors discussed the problem of micropolar fluid film lubrication between two parallel plates with reference to human joints. One of the recent but excellent papers demonstrating the basic theories of micropolar fluids and its applications is that given by Lukaszewicz [12]. Tulasi *et al.* [19] have investigated the convective heat and mass transfer flow of a micropolar fluid through a porous medium in a vertical channel by employing Galerkin finite element technique. Kumar *et al.* [11] have discussed the finite element solution of mixed convection micropolar fluid flow between two vertical plates with varying temperature. Sulochana *et al.* [18] have discussed the Soret effect and radiation absorption on convective heat and mass transfer flow of a micropolar fluid in a vertical channel with variable temperature.

In all the above works, the effect of thermal radiation on the flow characteristics has not been provided. The effect of radiation on MHD flow, heat and mass transfer problems has become important industrially. Abo-eldohad and Ghomaim (1) analysed the radiation effects on heat transfer of a micropolar fluid through a porous medium. Rahman and Sultana [14] have studied the steady convective flow of a micropolar fluid past a vertical porous flat plate in the presence of radiation with variable heat flux in porous medium.

From the scientific point of view, flow arising from temperature and material difference is applied in chemical engineering, geothermal reservoirs, aeronautics and astrophysics. In some applications, magnetic forces are present, and at other times, the flow is further complicated by the presence of radiation absorption, an excellent paradigm of this is in the planetary atmosphere where there is radiation absorption from nearby stars. Umadevi and Malasetty [20] have studied the problem of combined mixed convection flow in a vertical channel with symmetric and asymmetric boundary heating in the presence of viscous and joulean dissipations. The effect of chemical reaction and radiation absorption in the unsteady MHD free convection flow past a semi-infinite vertical permeable moving plate with a heat source and suction were studied [10,17]. Satyanarayana *et al.* [16] have discussed the effects of Hall current and radiation absorption on MHD micropolar fluid in a rotating system.

2. FORMULATION OF THE PROBLEM

We analyse a fully developed laminar convective heat and mass transfer flow of a viscous, electrically conducting micropolar fluid through a porous medium confined in a vertical channel bounded by flat walls. We choose a Cartesian co-ordinate system O (x, y, z) with x- axis in the vertical direction and y-axis normal to the walls. 'u' is the velocity component along the x-axis the component of micro rotation, T-the temperature and C –the concentration. Temperature is varying linearly along the x-axis with cx and mcx being the temperature of the left (y=0) and the right hand plate (y=+L) respectively while the walls are maintained at constant concentration. The porous medium is assumed to be isotropic and homogeneous with constant porosity and effective thermal diffusivity. The thermo physical properties of porous matrix are also assumed to be constant and Boussinesq approximation is invoked by confining the density variation to the buoyancy term. In the absence of any extraneous force flow is unidirectional along the x-axis which is assumed to be infinite.

The governing equations of this type of flow with thermal radiation (4) and Boussinesqu approximation are
Momentum:

$$(\mu + k)\frac{d^2u}{dy^2} + k\frac{d\omega}{dy} - \frac{dP}{dx} + \rho_e g(\beta T + \beta^* C) - \left(\frac{\mu}{k}\right)u - \left(\frac{\sigma\mu_e^2 H_o^2}{\rho_e}\right)u = 0 \tag{1}$$

Angular Momentum:

$$\gamma\frac{d^2\omega}{dy^2} - k\frac{du}{dy} - 2k\omega = 0 \tag{2}$$

Energy equation:

$$k_f \frac{d^2T}{dy^2}+\left(\mu+\frac{k}{2}\right)\left(\frac{du}{dy}\right)^2+\frac{k}{2}\left(\frac{du}{dy}+2\omega\right)^2+\gamma\left(\frac{d\omega}{dy}\right)^2-Q_H T+\frac{D_m K_T}{C_s C_p}\frac{d^2C}{dy^2}+\frac{16\sigma^{\bullet}T_\infty^3}{3\beta_R}\frac{\partial^2 T}{\partial y^2}=0 \quad (3)$$

Diffusion equation:

$$D_m\frac{d^2C}{dy^2}-k_c C+\frac{D_m K_T}{T_m}\frac{d^2T}{dy^2}=0 \quad (4)$$

$$N(x,o)=-s\left(\frac{\partial u}{\partial y}\right)_{y=0} \quad (5)$$

where s is the surface condition parameter and varies from 0 to 1.

The appropriate physical boundary conditions are given by

$$\begin{aligned} &u=0 \quad , \ \omega=\omega_o \qquad T=cx \qquad C=C1 \qquad on \quad y=-L \\ &u=0 \quad , \ \omega=\omega_o \qquad T=cmx \qquad C=C2 \qquad on \quad y=+L \end{aligned} \quad (6)$$

where m is the wall temperature ratio parameter and c is the varying temperature.

Introducing the dimensionless functions f, g, θ and ϕ. defined by

$$\eta=\frac{y}{L}, u=\frac{U_0}{S}f, T=\frac{cL}{S}\theta, C=\frac{L}{S}\phi, N=\frac{U_o}{LS}g, U_0=\frac{\rho\beta g_e L^3 c}{\mu}, S=\frac{\mu U_o^2}{k_f cl} \quad (7)$$

Where x, y, u, T, C, μ, k, D_m K_T T_m, Cp, Cs, L, Uo, β, β^*, No, N1, θ, ϕ, ω, η, C1, C2, kf, s, Q_H, $Q_1^{'}$ are defined in the Nomenclature of the thesis.

The set of differential equations (1)-(4) can be written in the following form:

$$(1+\Delta)\frac{d^2 f}{d\eta^2}+\Delta\frac{dg}{d\eta}+(\theta+N\varphi)-(D^{-1}+M^2)f=\frac{\mu U_o^2}{k_f\rho g_e\beta(cL)^2}\frac{dP}{dx} \quad (8)$$

$$A\frac{d^2 g}{d\eta^2}-\frac{df}{d\eta}-2g=0 \quad (9)$$

$$\left(1+\frac{4Rd}{3}\right)\frac{d^2\theta}{d\eta^2}+\left(1+\frac{R}{2}\right)\left(\frac{df}{d\eta}\right)^2+\frac{\Delta}{2}\left(\frac{df}{d\eta}+2g\right)^2+A\Delta\left(\frac{dg}{d\eta}\right)^2-\alpha\theta+Du\frac{d^2\phi}{d\eta^2}=0 \quad (10)$$

$$\frac{d^2\varphi}{d\eta^2}-\gamma\varphi+ScSo\frac{d^2\theta}{d\eta^2}=0 \quad (11)$$

Where R=k/μ is the dimensionless micropolar parameter, $A=\frac{\gamma}{kL^2}$ is the dimensionless micro rotation parameter, $\Delta P=\frac{\mu U_o^2}{k_f\rho g_e\beta(cL)^2}\frac{dP}{dx}$ is the pressure gradient parameter, $D^{-1}=\frac{L^2}{k_1}$ Is the Darcy parameter, $Sc=\frac{\nu}{D_m}$ is the Schmidt number, $N=\frac{\beta^*\Delta C}{\beta\Delta T}$ is the buoyancy ratio , $Rd=\frac{4\sigma^{\bullet}T_e^3}{\beta_R k_f}$ is the radiation parameter, $Q1=\frac{Q(C_1-C_2)L^{2'}}{C_p(T_1-T_2)}_1$ is the radiation absorption parameter, $So=\frac{D_m K_T(T_1-T_2)}{T_m(C_1-C_2)}$ is the Soret parameter, $Du=\frac{D_m K_T(C_1-C_2)}{C_s C_p(T_1-T_2)}$ is the Dufour parameter. The condition: $\Delta P=0\rightarrow\frac{dp}{dx}=0$ corresponds to a free convection flow, while non-zero values of the pressure gradient corresponds to a mixed convection flow.

The transformed boundary conditions are

$$f = 0 \ , \ g = \frac{LS}{U_o} N_0 = g_o, \theta = \frac{x}{L} S \ , \ C = 1 \quad on \ \eta = -1$$
$$f = 0 \ , \ g = \frac{LS}{U_o} N_0 = g_o, \theta = m\frac{x}{L} S \ , \ C = 0 \quad on \ \eta = +1 \tag{12}$$

The differential equations (8)-(11) with the boundary conditions as those given in (12) have been solved numerically using the finite element technique for the different parameters, namely the pressure gradient parameter ΔP , micropolar parameter R, Surface condition parameter go, Magnetic parameter M, Darcy parameter D^{-1}, Schmidt number Sc, heat source parameterα, Radiation parameter Rd, Radiation absorption parameter Q1, Soret parameter, So, Dufour parameter Duand the variable x.

3. METHOD OF SOLUTION

Finite element Method:

The set of differential equations given in equations (5.8)-(5.11) are highly nonlinear therefore it cannot be solved analytically. Hence, finite element analysis has been used in obtaining their solution. The steps involved in the finite element method are as follows:

1. Division of the domain into linear elements, called the finite element mesh.
2. Generation of the element equations using variation formulations.
3. Assembly of the element equations as obtained in steps (2).
4. Introduction of the boundary conditions to the equations obtained in (3).
5. Solution of the assembled algebraic equations.

To solve these differential equations with the corresponding boundary conditions, we assume if $f^i, g^i, \theta^i, \phi^i$ the approximations of f are, g, θ and ϕ we define the errors (residual) $E_u^i, E_g^i, E_\theta^i, E_\phi^i$ as

$$E_u^i = (1+R)\frac{d}{d\eta}\left(\frac{df^i}{d\eta}\right) + R\frac{dg^i}{d\eta} + (\theta^i + N\varphi^i) - (D^{-1} + M^2) f^i - \Delta P \tag{13}$$

$$E_g^i = A\frac{d}{d\eta}\left(\frac{dg^i}{d\eta}\right) - \frac{df^i}{d\eta} - 2g^i \tag{14}$$

$$E_\theta^i = \left(1 + \frac{4Rd}{3}\right)\frac{d}{d\eta}\left(\frac{d\theta^i}{d\eta}\right) + \left(1 + \frac{R}{2}\right)\left(\frac{df^i}{d\eta}\right)^2 + \frac{R}{2}\left(\frac{df^i}{d\eta} + 2g^i\right)^2 + AR\left(\frac{dg^i}{d\eta}\right)^2 - \alpha\theta^i + Du\frac{d}{d\eta}\left(\frac{d\phi^i}{d\eta}\right) \tag{15}$$

$$E_\varphi^i = \frac{d}{d\eta}\left(\frac{d\varphi^i}{d\eta}\right) - \gamma\varphi^i + ScSo\frac{d}{d\eta}\left(\frac{d\theta^i}{d\eta}\right) \tag{16}$$

Where,

$$\left.\begin{aligned} f^i &= \sum_{k=1}^{3} f_k \psi_k \\ g^i &= \sum_{k=1}^{3} g_k \psi_k \\ \theta^i &= \sum_{k=1}^{3} \theta_k \psi_k \end{aligned}\right\}$$
$$\varphi^i = \sum_{k=1}^{3} \varphi_k \psi_k \tag{17}$$

These errors are orthogonal to the weight function over the domain of e^i under Galerkin finite element technique we choose the approximation functions as the weight function.

The global matrix equations are coupled and are solved under iterative procedures until two consecutive iterations differ by a pre-assigned percentage.

4. SHEAR STRESS, NUSSELT NUMBER AND SHERWOOD NUMBER

The shear stress on the boundaries $y = 0,1$ in the non-dimensional form is $\tau_{y=0,1} = \left(\frac{df}{dy}\right)_{y=-1,,1}$

The rate of micro rotation (Couple stress)on the boundaries $y = 0,1$ in the non-dimensional form is

$$Cw_{y=0,1} = \left(\frac{dg}{dy}\right)_{y=-1,1}$$

The rate of heat transfer (Nusselt Number) is given by $Nu_{y=0,1} = \left(\frac{d\theta}{dy}\right)_{y=0,1}$

The rate of mass transfer (Sherwood Number) is given by $Sh_{y=0,1} = \left(\frac{d\phi}{dy}\right)_{y=-1,1}$

5. RESULTS AND DISCUSSION

The velocity, micro rotation, temperature and concentration have been evaluated by employing the finite element method and the results as shown graphically in Fig. 1a – 9a. The values of material constants S, L are taken to be fixed at 1.0 each while m is kept to be fixed at 2.0 and the effect of other important parameters, namely pressure gradient parameter Δp, surface condition go, chemical reaction parameter γ, thermal radiation parameter Rd, Dufour parameter Du and axial distance x.

The effect of chemical reaction of the velocity, micro-rotation, temperature and concentration can be seen from figs.1a-1d. From the profiles we notice that the velocity ,temperature enhances in the degenerating chemical reaction case and reduces in the generating chemical reaction case in the entire channel(figs.1a&1c). The couple stress enhances in the in the left half and reduces in the right half of the channel (fig.1b). The actual concentration reduces in the let half and enhances in the right half in the degenerating chemical reaction case while in the generating case, it enhances in the left half and reduces in the right half of the channel (fig.1d).The skin friction enhances at η=-1, couple stress enhances at η=+1, Nuselt number enhances at η=-1, Sherwood number enhances at $\eta = \pm 1$ with increase in γ in both degenerating and generating chemical reaction cases. The couple stress and Nusselt number reduces with γ at η=-1 in both the cases. The skin friction at η=+1 enhances in the degenerating chemical reaction case and reduces in the generating case (table.1)

The influence of thermo-diffusion and diffusion – thermo on f, ω, θ, ϕ can be seen from figs.2a-2d. From the profiles we notice that higher the thermo-diffusion effects (or lesser diffusion –thermo effects) smaller the velocity, temperature and concentration in the entire flow region (fig.2a, 2c, 2d). The micro-rotation experiences an enhancement in the left half and a depreciation in the right half of the channel (2b).This is owing to the fact that the thickness of the thermal and solutal boundary layers reduces with increase in Sr (or decreasing in Du). The skin friction enhances and the couple stress, Nusselt number reduces at η=-1 and at η=+1, the skin friction reduces and the couple stress, Nusselt number enhances with increase in Sr (or decrease in Du). The Sherwood number enhances at both the walls with increase in Sr(or decrease in Du) (table.1).

Figs.3a-3d shows the variation of f,ω,θ,ϕ with radiation parameter(Rd).From the figures we find that higher the radiative heat flux larger the micro-rotation and concentration in the left half and smaller in the right half of the channel.(figs.3b&3d).The velocity and temperature reduces with increase in Rd in the entire flow region(figs.3a&3c). There is a significant fall in the velocity and temperature in the presence of thermal radiation throughout the boundary layers. Further increase in thermal radiation parameter Rd results in the decrease of the velocity. The radiation parameter is found to decrease the hydrodynamic boundary layer along x-axis. Also as the Rosseland radiative absorption parameter enhances the corresponding heat flux converges and thus falling the rate of radiative heat transfer to the fluid causing a fall in the temperature of the fluid. The skin friction enhances and the couple stress reduces at η=-1while at η=+1, they exhibit a reversed behaviour with increasing radiation parameter Rd. The Nusselt and Sherwood number reduces at both the walls with Rd (table.1)

An increasing Q1 or Pr enhances a velocity (f) and reduces the concentration (C). The angular velocity reduces in the left half with Q1 and enhances with Pr and reversed effect is noticed in the right half of the channel. The temperature (θ) enhances in the left half and reduces the right half with Q1 while it enhances with Pr in the channel flow region (Fig. 4a-4d & 5a-5d).

An increase in x leads to an increase in the velocity (f) and temperature in the entire flow region (Figs. (6a, 6c). An increase in the axial distance x. The micro-rotation reduces in the left half and enhances in the right half of the channel with increase in x(6b). Also an increase in x enhances the concentration(fig.6d). The rate of micro rotation (Cw) enhances with increase in x at η= -1.At η=+1, Cw reduces with x. Nu enhances with increase in R at both the walls .With respect to micro rotation parameter x. The skin friction and Nusselt number reduces at η=-1 and enhances at η=1 with increase in x. The rate of mass transfer (Sherwood number reduces with x at η =-1& 1(table.1)

The effect of surface condition parameter (go) on f, ω, θ, ϕ can be shown in figs.7a-7d fixing the other parameters. It id found that an increase in go>0, leads an enhancement in the velocity f, and reduces with |go| in the entire channel. The couple stress enhances with go>0 and reduces with go<0 in the entire channel region (7b). The temperature enhances and actual concentration reduces with increase surface condition parameter go in the entire flow region (figs.7c&7d). It is also clear the Fig. 7b that for the positive values g_0, micro rotation increases continuously, until it reaches the maximum and then decreases continuously, while with the negative value of g_0, micro rotation decreases continuously until it reaches the minimum and then increases continuously. Thus, the pattern is different for negative and positive values of g_0. The skin friction, couple stress, Nusselt number and Sherwood number enhances at the left wall with increase in |go|. At the right wall, the Nusselt and Sherwood Number enhances and the couple stress reduces with increase in |go| (table.1)

The effect of micropolar parameter (A) on velocity, micro-rotation, temperature and concentration can be seen from graphs.8a-8d. It can be seen from the profiles that the velocity, micro-rotation enhances and the temperature reduces in the entire channel with increase in A (fig.8a-8c). The actual concentration reduces in the left half and enhances in the right half of the channel with increase in A (fig.8d). The skin friction enhances and the couple stress reduces at $\eta = \pm 1$. The Nusselt number and Sherwood number reduces at η= -1 with increase in A≤1.5 and enhances with higher A≥1.5 and at η=+1, they enhance with A. (table.1)

The effect of pressure gradient on velocity, mocro-rotation, temperature and concentration is exhibited in figs.9a-9d. It can be observed from the profiles that the velocity decreases with increase in pressure gradient. The micro-rotation and concentration enhances in the left half and reduces in the right half of the channel with ΔP (figs.9b&9d). The temperature reduces in the left half and enhances in the right half of the channel with increase in ΔP. (fig.9c). The skin friction enhances at η=-1 and reduces at η=1. The couple stress, Nusselt and Sherwood numbers reduce at the left wall and enhances at the right wall with increase in pressure gradient. (table.1)

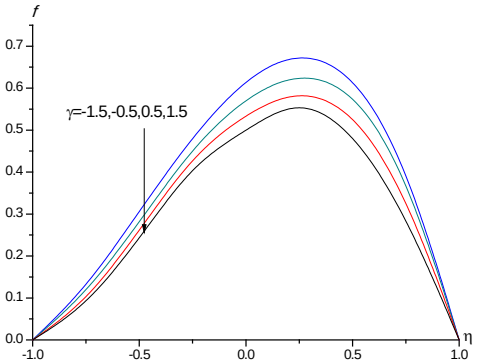

Fig.1a Variation of velocity(f) with γ
Sr=2,Du=0.03,Q1=0.5, Pr=0.71,Rd=0.5,A=0.5,Δ=1,Δp=1

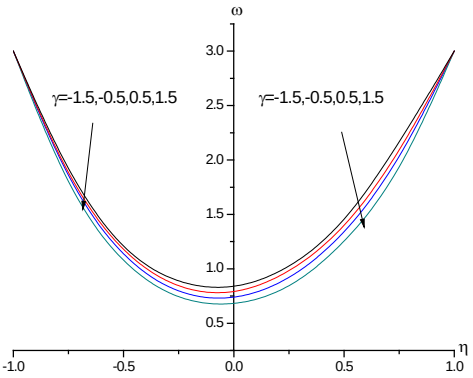

Fig.1b Variation of micro-rotation(ω) with γ
Sr=2,Du=0.03,Q1=0.5, Pr=0.71,Rd=0.5,A=0.5,Δ=1,Δp=1

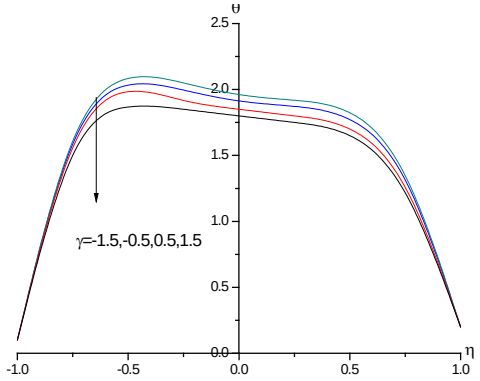

Fig.1c Variation of micro-rotation(θ) with γ
Sr=2,Du=0.03,Q1=0.5, Pr=0.71,Rd=0.5,A=0.5,Δ=1,Δp=1

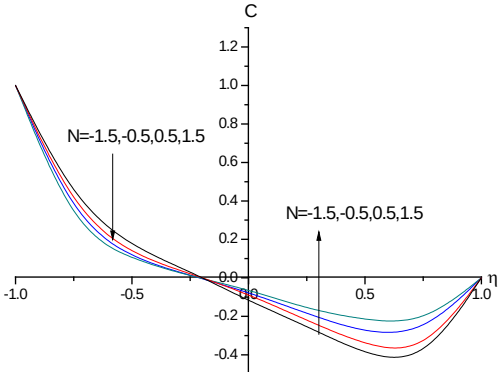

Fig.1d Variation of micro-rotation(C) with γ
Sr=2,Du=0.03,Q1=0.5,go=3,x=1,Pr=0.71,Rd=0.5,A=0.5,Δp=1

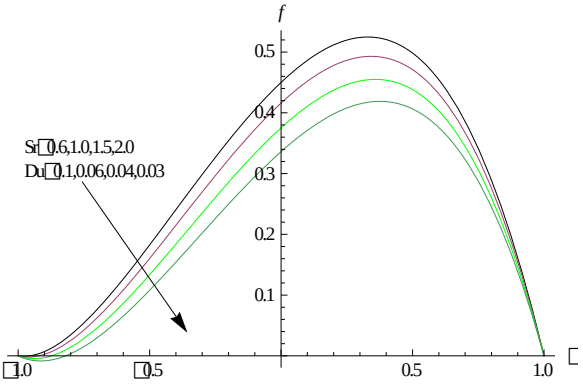

Fig.2a Variation of velocity(f) with Sr&Du
Sr=2,Du=0.03,Q1=0.5,go=3,x=1,Pr=0.71,Rd=0.5,A=0.5,Δp=1

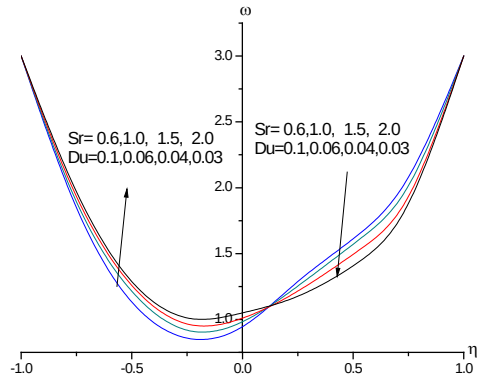

Fig.2b Variation of micro-rotation(ω) with Sr&Du
Sr=2,Du=0.03,Q1=0.5,go=3,x=1,Pr=0.71,Rd=0.5,A=0.5,Δp=1

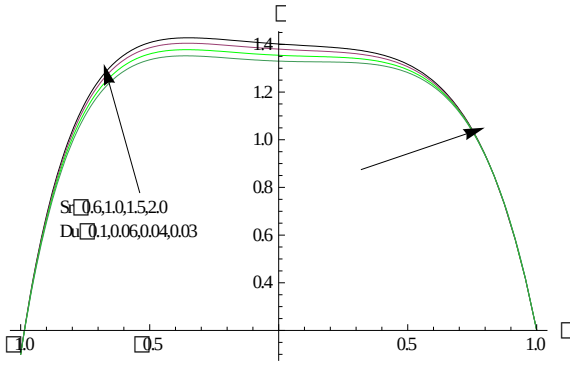

Fig.2c Variation of micro-rotation(θ) with Sr&Du
Sr=2,Du=0.03,Q1=0.5,go=3,x=1,Pr=0.71,Rd=0.5,A=0.5,Δp=1

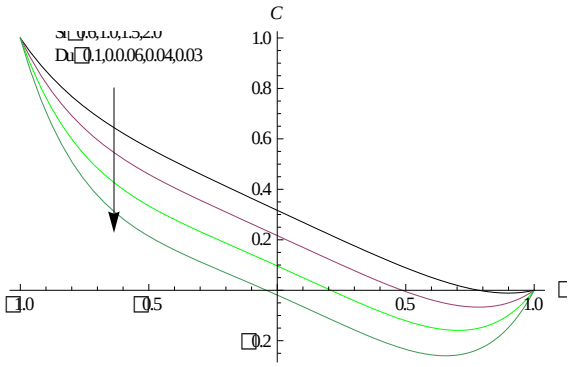

Fig.2d Variation of micro-rotation(C) with Sr&Du
Sr=2,Du=0.03,Q1=0.5,go=3,x=1,Pr=0.71,Rd=0.5,A=0.5,Δp=1

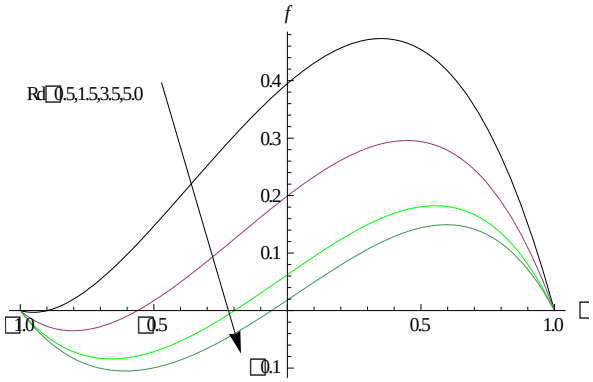

Fig.3a Variation of velocity(f) with Rd
Sr=2,Du=0.03,Q1=0.5, Pr=0.71,γ=0.5,A=0.5,Δp=1

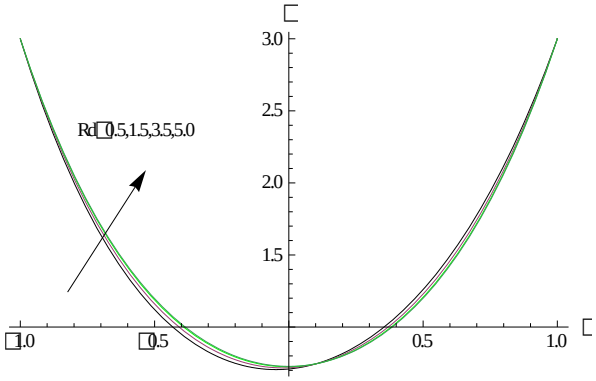

Fig.3b Variation of micro-rotation(ω) with Rd
Sr=2,Du=0.03,Q1=0.5, Pr=0.71,γ=0.5,A=0.5,Δp=1,

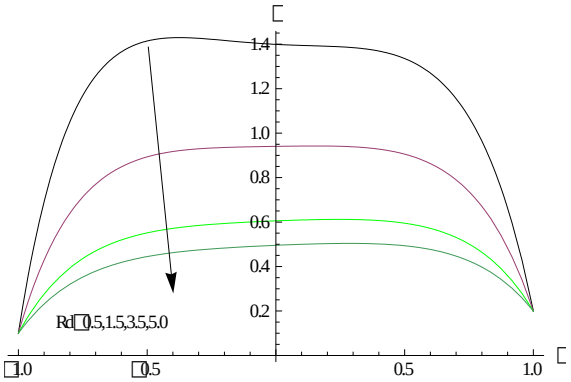

Fig.3c Variation of micro-rotation(θ) with Rd
Sr=2,Du=0.03,Q1=0.5, Pr=0.71,γ=0.5,A=0.5,Δp=1,

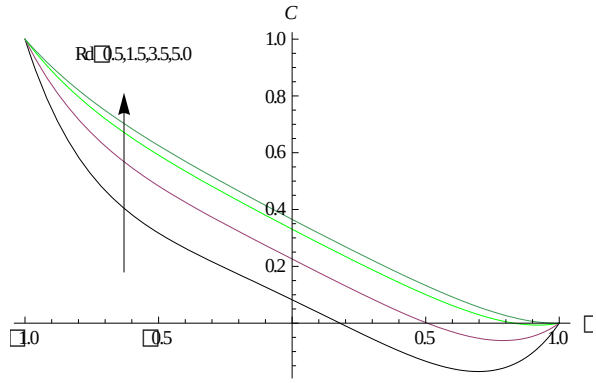

Fig.3d Variation of micro-rotation(C) with Rd
Sr=2,Du=0.03,Q1=0.5, Pr=0.71,γ=0.5,A=0.5,Δp=1,

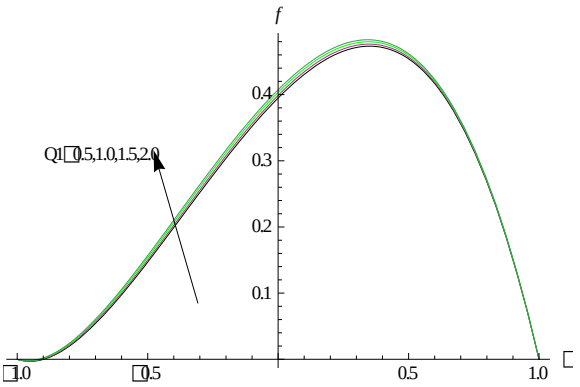

Fig.4a Variation of velocity(f) with Q1
Sr=2,Du=0.03,γ=0.5, Pr=0.71,Rd=0.5,A=0.5,Δp=1

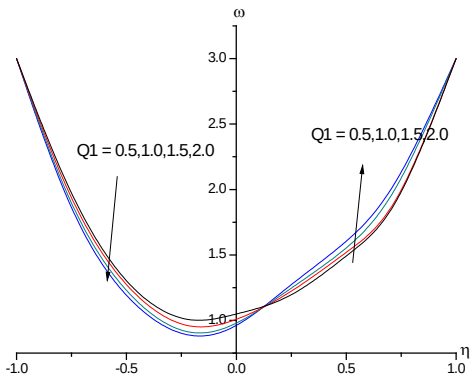

Fig.4b Variation of micro-rotation(ω) with Q1
Sr=2,Du=0.03,γ=0.5, Pr=0.71,Rd=0.5,A=0.5,Δp=1

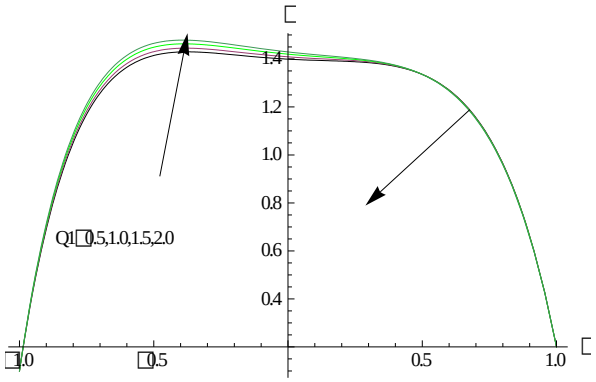

Fig.4c Variation of micro-rotation(θ) with Q1
Sr=2,Du=0.03,γ=0.5, Pr=0.71,Rd=0.5,A=0.5,Δp=1

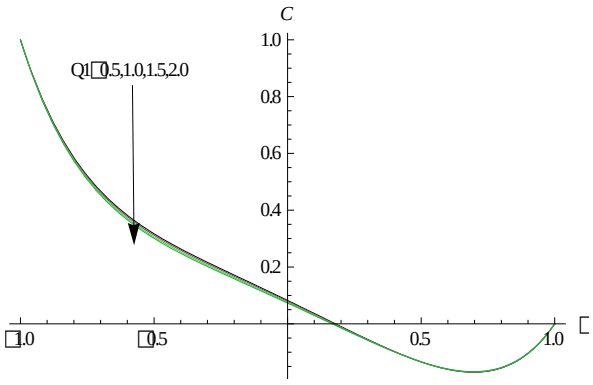

Fig.4d Variation of micro-rotation(C) with Q1
Sr=2,Du=0.03,γ=0.5, Pr=0.71,Rd=0.5,A=0.5,Δp=1

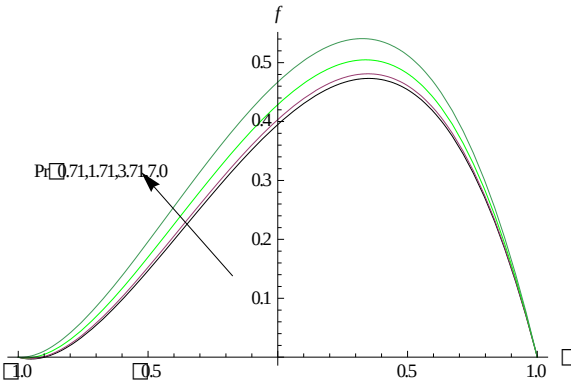

Fig.5a Variation of velocity(f) with Pr
Sr=2,Du=0.03,Q1=0.5,,γ=0.5,Pr=0.71,Rd=0.5,A=0.5,Δp=1

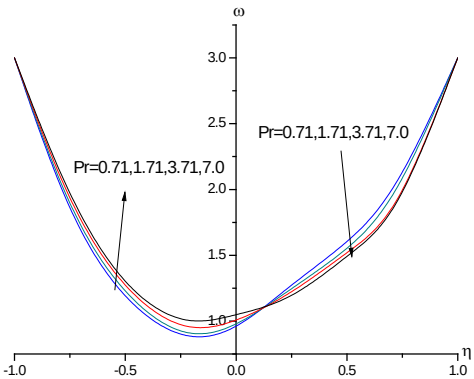

Fig.5b Variation of micro-rotation(ω) with Pr
Sr=2,Du=0.03,Q1=0.5,,γ=0.5,Pr=0.71,Rd=0.5,A=0.5,Δp=1

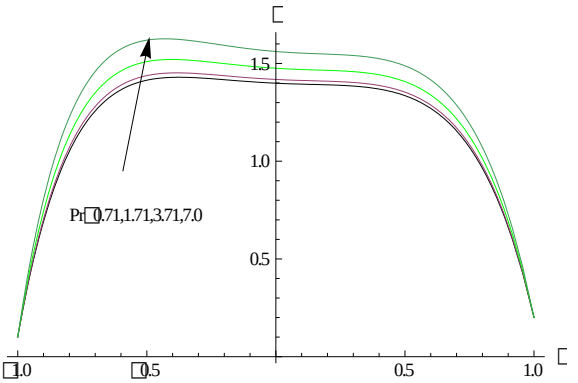

Fig.5c Variation of micro-rotation(θ) with Pr
Sr=2,Du=0.03,Q1=0.5,,γ=0.5,Pr=0.71,Rd=0.5,A=0.5,Δp=1

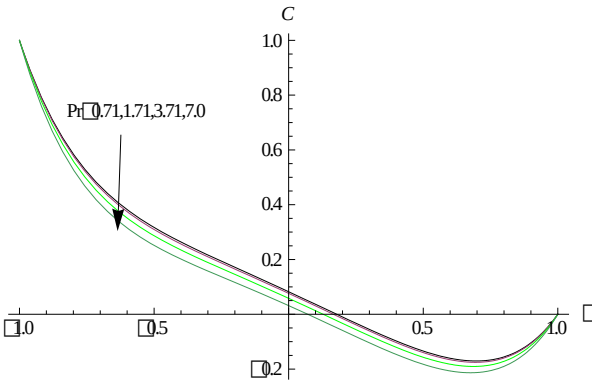

Fig.5d Variation of micro-rotation(C) with Pr
Sr=2,Du=0.03,Q1=0.5,,γ=0.5,Pr=0.71,Rd=0.5,A=0.5,Δp=1

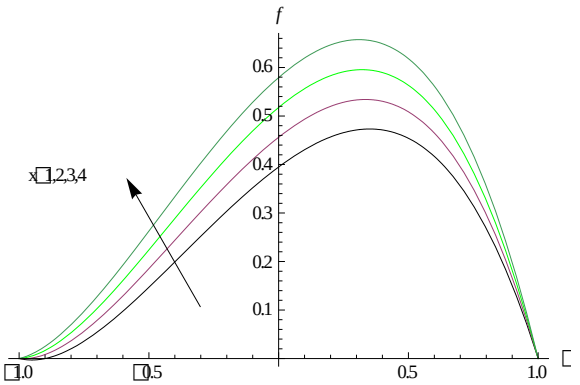

Fig.6a Variation of velocity(f) with x
Sr=2,Du=0.03,Q1=0.5,γ=0.5,Pr=0.71,Rd=0.5,A=0.5,Δp=1

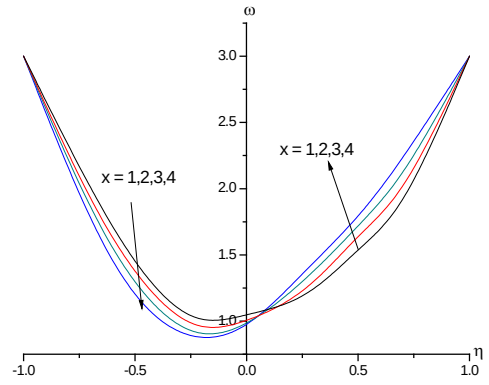

Fig.6b Variation of micro-rotation(ω) with x
Sr=2,Du=0.03,Q1=0.5,γ=0.5,Pr=0.71,Rd=0.5,A=0.5,Δp=1

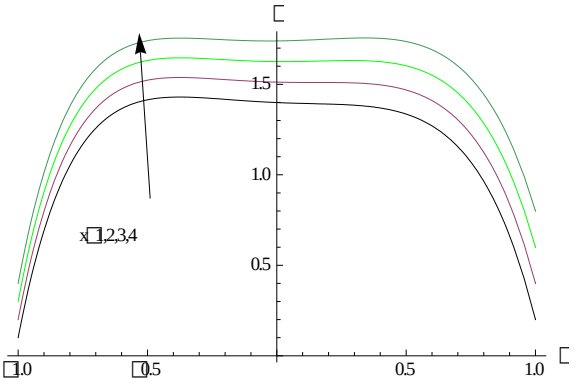

Fig.6c Variation of micro-rotation(θ) with x
Sr=2,Du=0.03,Q1=0.5,γ=0.5,Pr=0.71,Rd=0.5,A=0.5,Δp=1

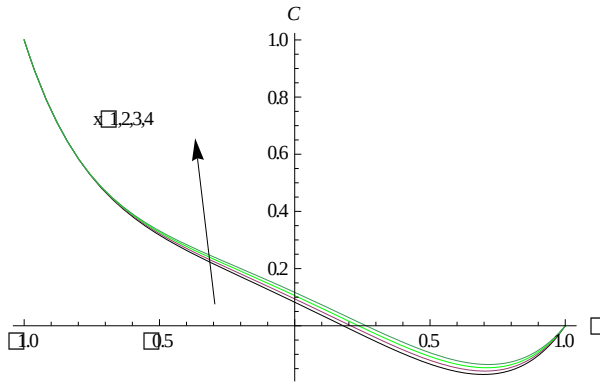

Fig.6d Variation of micro-rotation(C) with x
Sr=2,Du=0.03,Q1=0.5,γ=0.5,Pr=0.71,Rd=0.5,A=0.5,Δp=1

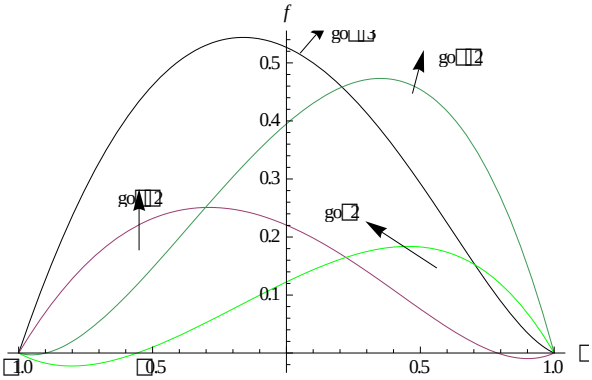

Fig.7a Variation of velocity(f) with go
Sr=2,Du=0.03,Q1=0.5,γ=0.5,Pr=0.71,Rd=0.5,A=0.5,Δp=1

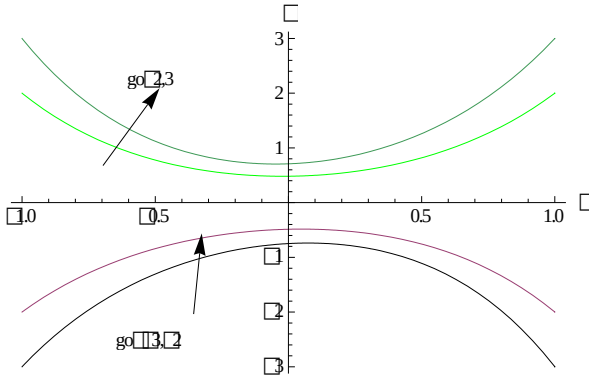

Fig.7b Variation of micro-rotation(ω) with go
Sr=2,Du=0.03,Q1=0.5,γ=0.5,Pr=0.71,Rd=0.5,A=0.5,Δp=1

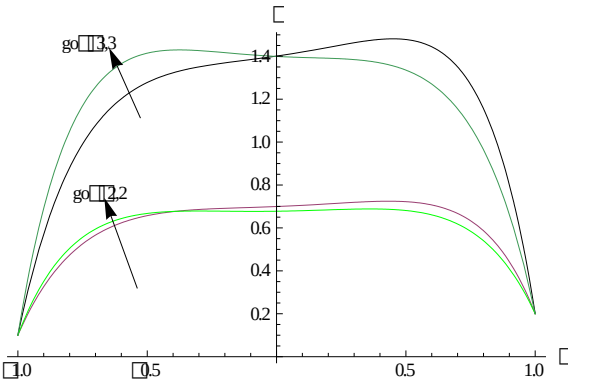

Fig.7c Variation of micro-rotation(θ) with go
Sr=2,Du=0.03,Q1=0.5,γ=0.5,Pr=0.71,Rd=0.5,A=0.5,Δp=1

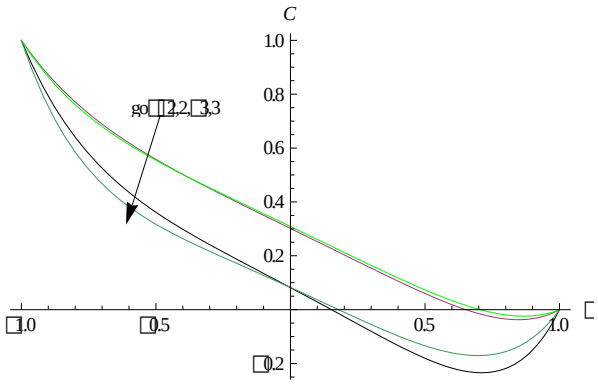

Fig.7d Variation of micro-rotation(C) with go
Sr=2,Du=0.03,Q1=0.5,γ=0.5,Pr=0.71,Rd=0.5,A=0.5,Δp=1

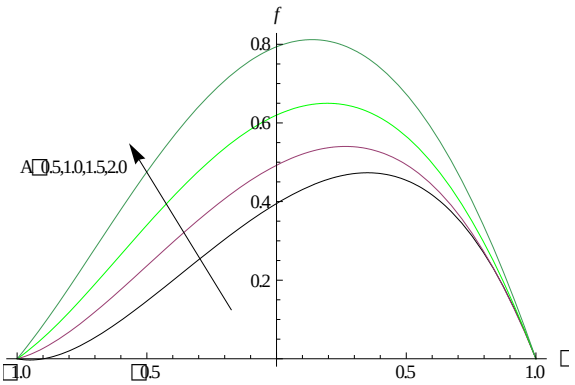

Fig.8a Variation of velocity(f) with A
Sr=2,Du=0.03,Q1=0.5, Pr=0.71,Rd=0.5,γ=0.5,Δp=1

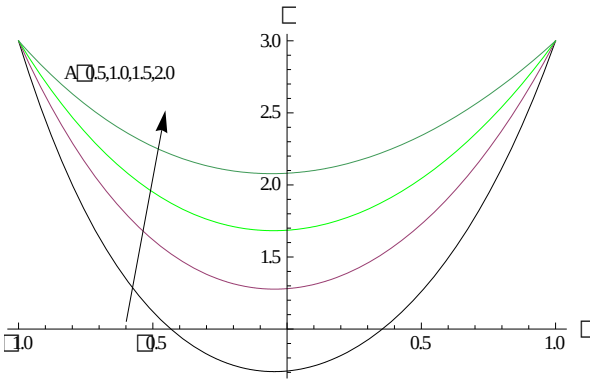

Fig.8b Variation of micro-rotation(ω) with A
Sr=2,Du=0.03,Q1=0.5, Pr=0.71,Rd=0.5,γ=0.5,Δp=1

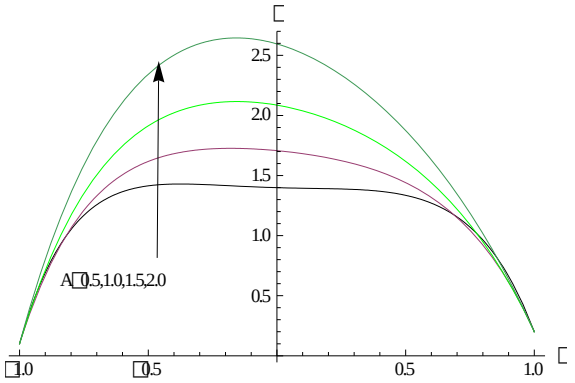

Fig.8c Variation of micro-rotation(θ) with A
Sr=2,Du=0.03,Q1=0.5, Pr=0.71,Rd=0.5,γ=0.5,Δp=1

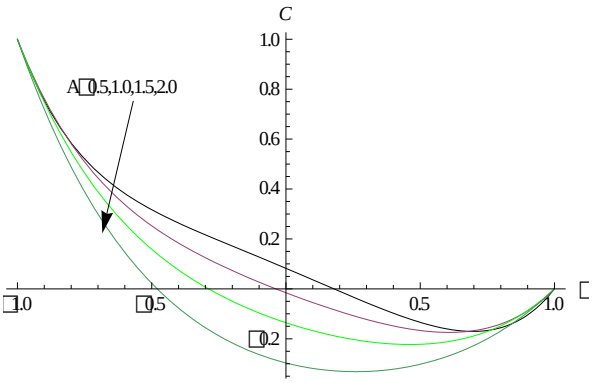

Fig.8d Variation of micro-rotation(C) with A
Sr=2,Du=0.03,Q1=0.5, Pr=0.71,Rd=0.5,γ=0.5,Δp=1

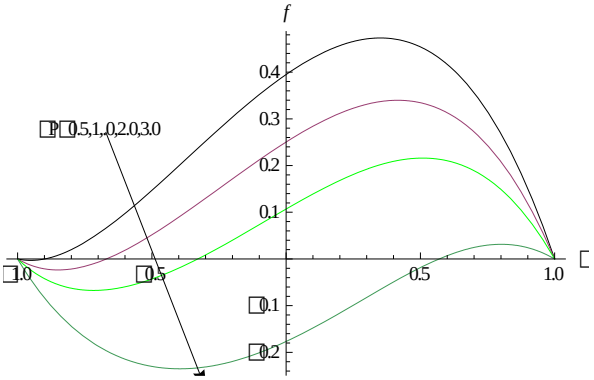

Fig.9a Variation of velocity(f) with Δp
Sr=2,Du=0.03,Q1=0.5,Pr=0.71,Rd=0.5,A=0.5,γ=0.5

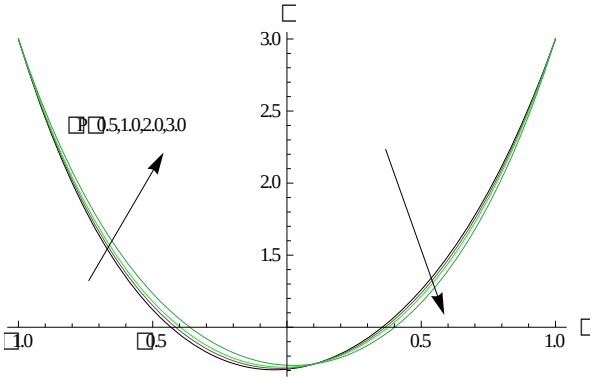

Fig.9b Variation of micro-rotation(ω) with Δp
Sr=2,Du=0.03,Q1=0.5,Pr=0.71,Rd=0.5,A=0.5,γ=0.5

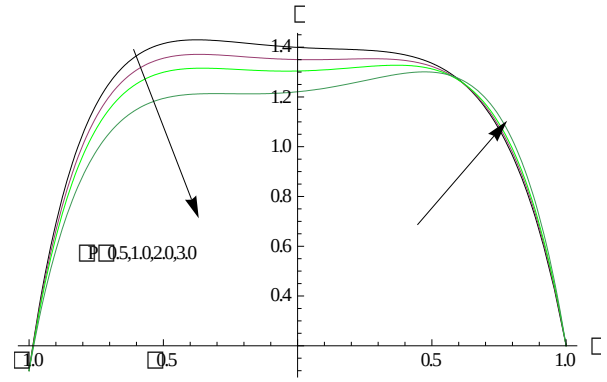

Fig.9c Variation of micro-rotation(θ) with ΔP
Sr=2,Du=0.03,Q1=0.5,Pr=0.71,Rd=0.5,A=0.5,γ=0.5

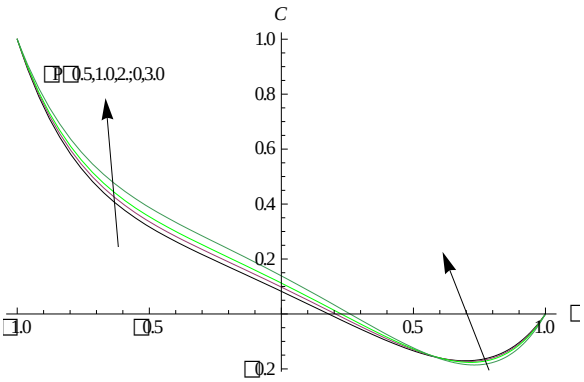

Fig.9d Variation of micro-rotation(C) with Δp
Sr=2,Du=0.03,Q1=0.5,Pr=0.71,Rd=0.5,A=0.5,γ=0.5

Table-1: Shear Stress, Couple Stress, Nusselt Number and Sherwood Number at $\eta = \pm 1$.

Parameter		τ(-1)	τ (1)	Cw(-1)	Cw(1)	Nu(-1)	Nu(1)	Sh(-1)	Sh(1)
Rd	0.5	-0.2041	-1.5588	-5.9985	5.26308	-6.9591	5.46877	3.56373	-1.918
	1.5	-0.4366	-1.2022	-5.8234	5.46282	-3.8933	3.39508	2.23305	-1.0221
	3.5	-0.5725	-0.9157	-5.6896	5.63022	-2.0787	1.93356	1.44737	-0.3911
	5	-0.8889	-0.2976	-5.4516	5.9316	-1.9935	1.18083	1.22996	-0.2459
γ	5.0	-0.2041	-1.5588	-5.9985	5.26308	-6.9591	5.46877	3.56373	-1.918
	1.5	-0.2288	-1.5803	-5.9811	5.27268	-3.8933	5.48521	3.59259	-1.9051
	-0.5	-0.2825	-1.6258	-5.9343	5.30623	-2.0787	5.53745	3.44743	-1.9688
	-1.5	-1.5122	0.00754	-5.1879	6.13629	-1.9935	5.91793	3.6222	-2.9463
Q1	0.5	-0.2041	-1.5588	-5.9985	5.26308	-6.9591	5.46877	3.56373	-1.918
	1	-0.2251	-1.578	-5.9826	5.27281	-6.9816	5.45947	3.57363	-1.914
	1.5	-0.2792	-1.624	-5.9358	5.30613	-6.9309	5.48689	3.55164	-1.9262
	2	-1.4714	-0.0336	-5.2097	6.11506	-7.9079	5.7651	3.69997	-2.7443
Sr/Du	0.6/0.1	-0.057	-1.7965	-6.1088	5.1357	-7.3049	5.37882	1.51387	-0.2374
	1.0/0.06	-0.131	-1.7529	-6.0565	5.18316	-7.1529	5.42057	2.1093	-0.7152
	1.5/0.04	-0.2467	-1.7161	-5.9654	5.26454	-6.9088	5.51149	2.82856	-1.3599
	2.0/0.03	-1.5136	-0.0111	-5.1906	6.12948	-5.8979	5.90754	3.66574	-2.833
Δp	0.1	-0.2041	-1.5588	-5.9985	5.26308	-6.9591	5.46877	3.56373	-1.918
	2	-0.6222	-0.8844	-5.7119	5.59884	-6.2722	5.91299	3.26524	-2.1151
	3	-0.9484	-0.1241	-5.4455	5.94955	-5.6608	6.44158	2.99976	-2.3493
	4	-2.1123	-0.0.1158	-4.6771	6.91629	-7.276	7.57095	3.07799	-3.4539
x	1.0	-0.2041	-1.5588	-5.9985	5.26308	-6.9591	5.46877	3.56373	-1.918
	2	-0.1188	-1.7341	-6.0583	5.18677	-7.0487	5.18261	3.58209	-1.8155
	3	-0.0332	-1.9099	-6.1182	5.11022	-7.1407	4.89986	3.60144	-1.7145
	4	-0.1064	-2.5894	-2.7613	4.78648	-2.0439	3.70961	1.31228	-1.2665
g_0	-3.0	1.28972	-0.0767	-5.2113	-6.1622	-5.591	7.11525	2.96404	-2.6395
	-2	0.73863	0.2618	3.58112	-3.9628	-2.6663	2.87063	1.70214	-0.7993
	2	-0.2819	-0.7361	-3.8808	3.65701	-2.9551	2.50111	1.82941	-0.6379
	3	-1.8893	-0.3123	-5.144	6.03636	-9.0287	5.73962	3.68975	-2.7887
A	0.2	-0.2041	-1.5588	-5.9985	5.26308	-6.9591	5.46877	3.56373	-1.918
	0.4	0.30573	-1.5838	-3.0262	2.60363	-6.4907	4.48861	3.3407	-1.4724
	0.6	0.33793	-1.7829	-2.4904	2.13537	-6.6974	4.55108	3.42455	-1.4934
	0.8	-2.083	1.12648	-1.72	2.09359	-11.468	5.04249	4.04335	-3.1168

6. CONCLUSIONS

- The velocity decreases with increase in pressure gradient. The micro-rotation and concentration enhances in the left half and reduces in the right half of the channel with Δp. The temperature reduces in the left half and enhances in the right half of the channel. The skin friction enhances at η=-1 and reduces at η=1. The couple stress, Nusselt and Sherwood number reduces at η=-1 and enhances at η=1 with increase in pressure gradient Δp.
- The velocity, micro-rotation, temperature and concentration enhances in the degenerating chemical reaction case and reduces in the generating chemical reaction case in the entire channel. The skin friction, Nusselt number reduces and Sherwood number, couple stress enhances at η=0 with γ>0. The friction and Sherwood number enhances at η=1 with γ>0. For γ<0, the skin friction enhances, couple stress, Number and Sherwood number reduces at η=0.At η=1,τ, Nu reduces and Cw and Sh enhances with increase in γ<0.

- An increase in the radiation absorption parameter Q_1 leads to an enhancement in the velocity, temperature and reduction in the concentration in the entire flow region. The micro-rotation reduces in the left half and enhances in the right half of the channel. An increase in the radiation absorption parameter Q_1 enhances $|Cw|$ at $\eta = 0$ and reduces at $\eta=1$ The rate of heat and mass transfer reduces at the left wall and enhances at the right wall
- Higher the thermo-diffusion effects (or lesser the diffusion –thermo effects) larger the micro-rotation and smaller the temperature and concentration in the flow region. The velocity reduces in the left half and enhances in the right half of the channel. The skin friction enhances, Nusselt and Sherwood number reduces with increase in Sr at the left wall. At the right wall, The skin friction, Sherwood number enhances, the couple stress, Nusselt number reduces at $\eta=0$ with increase in Sr (or decrease in Du). The skin friction and Nusselt number reduces, the couple stress, Sherwood number enhances at $\eta=1$ with Sr (or decrease in Du Higher the radiative heat flux larger the micro-rotation in left half and smaller micro-rotation in right half and larger concentration. The velocity, temperature reduces with Rd in the entire flow region. The Nuselt and Sherwood number reduces at both the walls with increase in Rd. The skin friction reduces at the left wall and enhances at the right wall with increase in Rd.
- An increase in go>0, leads an enhancement in the velocity f. An increase in go<0, reduces f in the flow region. The micro rotation increases with the increase of the surface condition parameter $g_{0>}0$ and reduces with go<0. The temperature enhances with increase in the absolute value of surface condition parameter $|g_0|$ .The Nusselt and Sherwood number enhances at the left wall with increase in go. At the right wall, the skin friction, couple stress, Nusselt and Sherwood number enhances with go.
- Cw, Nu and Sh reduces at the left wall and enhances at the right wall with Δp.
- The velocity, couple stress, temperature and concentration enhances with increase in micropolar parameter (A). The skin friction enhances at $\eta = 0$ and reduces at $\eta = 1$. The couple stress, Nusselt and Sherwood number reduces at $\eta = 0, 1$ with increase in A

7. REFERENCES

1. Abo-eldohad EM.Ghonaim AF: Radiation effect on heat transfer of a micropolar fluid through a porous medium., Appl.Math. Compt., V.169(1), pp.500-516 (2005)
2. Agarwal R.S. and Dhanpal C.: Numerical solutions of free convection micropolar fluid flow between two parallel porous vertical plates, Int. J. Engg. Sci. 26, 1247-1255, (1988).
3. Ariman T., Turk M.A. and Sylvester N.D.: Review article-Applications of micro continuum fluid mechanics, Int. J. Engg. Sci. 12, 273-293, (1974).
4. Bhargava R. and Rani M.: Numerical solution of heat transfer in micropolar fluid flow in a channel with porous walls, Int. J. Engng. Sci. 23, 409-413, (1985).
5. Chamkha A.J., Grosan T. and Pop I.: Fully developed free convection of a micropolar fluid in a vertical channel, Int. Comm. Heat and Mass Transfer, 29, 1119-1127, (2002).
6. Eringen A.C.: Simple micro fluids, Int. J. Eng. Sci. 2, 2052-217, (1964).
7. Eringen A.C.: Theory of micropolar fluids, J. Math. Mech. 16, 1-18, (1966).
8. Gorla R.S.R., Ghorashi B. and Wangskarn P.: Mixed convection in vertical internal flow of a micropolar fluid, Int. J. Engg. Sci. 27, 1553-1561, (1989).
9. Hoyt J.W. and Fabula A.G.: The effect of additives on fluid friction, U.S. Naval Ordnance Test Station Report, 1964.
10. Ibrahim F.S., Elaiw A.M., Bakr A.A.: Effect of the chemical reaction and radiation absorption on the unsteady MHD free convection flow past a semi-infinite vertical permeable moving plate with heat source and suction, communications in Non-linear Science and Numerical Simulation, 13, pp. 1056-1066 (2008).
11. Kumar L., Bhargava R., Bhargava P. and Takhar H.S.: Finite element solution of mixed micropolar fluid flow between two vertical plates with varying temperature. Arch. Mech., V. 57(4), pp. 251-264, (2005).
12. Lukaszewicz G.: Micro polar fluids-Theory and Applications, Birkhauser Boston, (1999).
13. Nigam K.M., Manohar K. and Joggi S.: Micropolar fluid film lubrication between two parallel plates with reference to human joints, Int. J. Mech. Sci. 24, 661-671, (1982).
14. Rahman MM,Sultana T :Radiation heat transfer flow of micropolar fluid with variable heat flux in a porous medium.,Nonlinear anal Model comtrol,V,13(1), pp.71-87(2008)
15. Sastry V.U.K. and Rao V.R.M.: Numerical solution of micropolar fluid flow in a channel with porous walls, Int. J. Eng. Sci., 20, 631-642, (1982).
16. Satyanarayana,P.V,Venkateswarlu,B and Venkataramana:Effects of Hall current and radiatiuon absorption on MHD micropolar fluid in a rotating
17. Srinivasacharya D., Murthy J.V.R. and Venugopalam D.: Unsteady stokes flow of micropolar fluid between two parallel porous plates, Int. J. Engng Sci., 39, 1557-1563, (2001).
18. Sulochana,c and Gnanaprasunamba,K: combined influence of chemical reaction and radiation absorption on mixed convective heat and mass transfer flow of a micropolar fluid through a porous medium in a vertical channel with varied temperature.,Int.J.Adv.Sci.Tech.res,V.3(5),pp.570-603(2015).

19. Tulasi Lakshmi Devi B. and Prasada Rao D.R.V.: Finite element analysis of convective heat transfer flow of a micropolar fluid through a porous medium in a vertical channel, Ph.D. Thesis, S.K. University, Anantapur, India
20. Umadevi JC, Malashetty MS: Magnetohydrodynamic mixed convection in a vertical channel., Int.J.Non-Linear Mech ., V.40),pp..91-101(2005).

Source of support: Nil, Conflict of interest: None Declared.